CRCLEME
Cooperative Research Centre for
Landscape Evolution & Mineral Exploration

CSIRO
EXPLORATION
AND MINING

AMIRA
Australian Mineral Industries Research Association Limited ACN 004 448 266

OPEN FILE
REPORT
SERIES

ELECTRON MICROPROBE STUDIES OF MINERALS FROM WEATHERED PROFILES, PARKINSON PIT AND ENVIRONS, MT MAGNET, WESTERN AUSTRALIA

K.M. Scott

CRC LEME OPEN FILE REPORT 25

September 1998

(CSIRO Division of Exploration Geoscience Report 147R, 1990.
Second impression 1998)

AMIRA
Australian Mineral Industries Research Association Limited ACN 004 448 266

CRCLEME
Cooperative Research Centre for
Landscape Evolution & Mineral Exploration

CSIRO
EXPLORATION
AND MINING

ELECTRON MICROPROBE STUDIES OF MINERALS FROM WEATHERED PROFILES, PARKINSON PIT AND ENVIRONS, MT MAGNET, WESTERN AUSTRALIA

K.M. Scott

CRC LEME OPEN FILE REPORT 25

September 1998

(CSIRO Division of Exploration Geoscience Report 147R, 1990.
Second impression 1998)

CRC LEME is an unincorporated joint venture between The Australian National University,
University of Canberra, Australian Geological Survey Organisation and CSIRO Exploration and Mining
Headquarters: CRC LEME c/o CSIRO Exploration and Mining, Private Bag, PO Wembley, Western Australia, 6014

RESEARCH ARISING FROM CSIRO/AMIRA REGOLITH GEOCHEMISTRY PROJECTS 1987-1993

In 1987, CSIRO commenced a series of multi-client research projects in regolith geology and geochemistry which were sponsored by companies in the Australian mining industry, through the Australian Mineral Industries Research Association Limited (AMIRA). The initial research program, "Exploration for concealed gold deposits, Yilgarn Block, Western Australia" (1987-1993) had the aim of developing improved geological, geochemical and geophysical methods for mineral exploration that would facilitate the location of blind, buried or deeply weathered gold deposits. The program included the following projects:

P240: Laterite geochemistry for detecting concealed mineral deposits (1987-1991). Leader: Dr R.E. Smith.
Its scope was development of methods for sampling and interpretation of multi-element laterite geochemistry data and application of multi-element techniques to gold and polymetallic mineral exploration in weathered terrain. The project emphasised viewing laterite geochemical dispersion patterns in their regolith-landform context at local and district scales. It was supported by 30 companies.

P241: Gold and associated elements in the regolith - dispersion processes and implications for exploration (1987-1991). Leader: Dr C.R.M. Butt.
The project investigated the distribution of ore and indicator elements in the regolith. It included studies of the mineralogical and geochemical characteristics of weathered ore deposits and wall rocks, and the chemical controls on element dispersion and concentration during regolith evolution. This was to increase the effectiveness of geochemical exploration in weathered terrain through improved understanding of weathering processes. It was supported by 26 companies.

These projects represented "an opportunity for the mineral industry to participate in a multi-disciplinary program of geoscience research aimed at developing new geological, geochemical and geophysical methods for exploration in deeply weathered Archaean terrains". This initiative recognised the unique opportunities, created by exploration and open-cut mining, to conduct detailed studies of the weathered zone, with particular emphasis on the near-surface expression of gold mineralisation. The skills of existing and specially recruited research staff from the Floreat Park and North Ryde laboratories (of the then Divisions of Minerals and Geochemistry, and Mineral Physics and Mineralogy, subsequently Exploration Geoscience and later Exploration and Mining) were integrated to form a task force with expertise in geology, mineralogy, geochemistry and geophysics. Several staff participated in more than one project. Following completion of the original projects, two continuation projects were developed.

P240A: Geochemical exploration in complex lateritic environments of the Yilgarn Craton, Western Australia (1991-1993). Leaders: Drs R.E. Smith and R.R. Anand.
The approach of viewing geochemical dispersion within a well-controlled and well-understood regolith-landform and bedrock framework at detailed and district scales continued. In this extension, focus was particularly on areas of transported cover and on more complex lateritic environments typified by the Kalgoorlie regional study. This was supported by 17 companies.

P241A: Gold and associated elements in the regolith - dispersion processes and implications for exploration. Leader: Dr. C.R.M. Butt.
The significance of gold mobilisation under present-day conditions, particularly the important relationship with pedogenic carbonate, was investigated further. In addition, attention was focussed on the recognition of primary lithologies from their weathered equivalents. This project was supported by 14 companies.

Although the confidentiality periods of the research reports have expired, the last in December 1994, they have not been made public until now. Publishing the reports through the CRC LEME Report Series is seen as an appropriate means of doing this. By making available the results of the research and the authors' interpretations, it is hoped that the reports will provide source data for future research and be useful for teaching. CRC LEME acknowledges the Australian Mineral Industries Research Association and CSIRO Division of Exploration and Mining for authorisation to publish these reports. It is intended that publication of the reports will be a substantial additional factor in transferring technology to aid the Australian Mineral Industry.

This report (CRC LEME Open File Report 25) is a Second impression (second printing) of CSIRO, Division of Exploration Geoscience Restricted Report 147R, first issued in 1990, which formed part of the CSIRO/AMIRA Project P241.

Copies of this publication can be obtained from:
The Publication Officer, c/- CRC LEME, CSIRO Exploration and Mining, PMB, Wembley, WA 6014, Australia. Information on other publications in this series may be obtained from the above or from http://leme.anu.edu.au/
Cataloguing-in-Publication:
Scott, K.M.
Electron microprobe studies of minerals from weathered profiles, Parkinson Pit and environs, Mt Magnet, WA
ISBN 0 642 28210 2
1. Weathering - Western Australia 2. Electron microprobe analysis 3. Geochemistry.
I. Title
CRC LEME Open File Report 25.
ISSN 1329-4768

TABLE OF CONTENTS

LIST OF TABLES

LIST OF FIGURES

Figure 8 Primary (i.e.Ag-rich) gold grains (white) in chlorite matrix (grey). Back Scattered Electron Image. Sample 105099. Scale ≡ 100 μm.

Figure 9 Complex primary gold grain (white) associated with phyllosilicates (grey). Back Scattered Electron Image. Sample 105099. Scale ≡ 100 μm.

Figure 10 Au Mα map for Figure 9 area.

Figure 11 Ag Lα map for Figure 9 area, indicating Ag-rich core to upper portion of gold grain.

SUMMARY

Major and trace element data for more than 100 minerals from 24 separate samples reveal the host minerals for specific elements during weathering processes at Mt Magnet.

Resistant minerals like rutile, spinel, tourmaline and mica retain their component elements through the weathering profile with a low Fe* (i.e. Fe/(Fe+Mg+Mn) ratio for muscovite and tourmaline indicating proximity to mineralization. Gold and talc are not so resistant to weathering, with gold losing its Ag content during weathering processes at Mt Magnet. Sulfides, chlorite, feldspars and carbonates are readily destroyed during weathering with their component elements either incorporated into Fe and Mn oxides, kaolinite and smectitic clay or lost to the profile by dispersal by groundwaters. The Fe oxides are particularly important hosts for Au-pathfinder elements (e.g. As, Sb and W). Chlorite, carbonate and sulfide compositions may reflect proximity to mineralization and be useful in deep profiles but because of their susceptibility to weathering they are not as versatile as mica or tourmaline.

The Cr contents of each of chlorite, muscovite, rutile and perhaps spinel, indicate the lithology of their host samples by showing decreasing Cr contents from ultramafic to mafic to felsic rocks.

1. INTRODUCTION

Two previous studies of weathered profiles at Mt Magnet (Scott 1989a, c) have detailed the major mineralogical and geochemical features in barren and mineralized mafic and felsic sequences. One of the features of these studies was the observation that the Na- and Ca-rich micas, paragonite and margarite, were only present in barren mafic sequences.

By the use of the electron microprobe, this study characterizes micas and other minerals more completely to determine whether specific minerals have compositional features which can be used to identify various lithologies and/or proximity to mineralization. The study also considers how the relative stability of various minerals effects elemental distributions through the weathered profile at Mt Magnet.

2. SAMPLES AND METHODS

A total of 24 samples were analysed by electron microprobe techniques. Of these 18 were from the pit area from the drill holes NMS D4, NMS D5, NMS D7, NMS D8 and NMS D9 and one was from a hand specimen of quartz-tourmaline vein from 405RL at 5847E/3890N. Five samples were from the drill holes PKN 039 and PKN 203, occurring up to 300 m to the west of the pit (Fig. 1).

All analyses were performed on a CAMECA electron microprobe. Silicate minerals (micas, chlorites, talc, kaolinite and tourmaline) and carbonates were analysed at 15 kV, 20 nA using a defocussed beam to prevent volatilization during analysis. Fe, Mn and Ti oxide phases and sulfides were analysed at 20 kV, 20 nA. Each of the 10-12 elements forming part of an analytical array for these analyses was counted for 20 seconds and two background positions for 10 seconds.

Trace element arrays consisting of 4-6 elements allowed concentrations down to 100 ppm to be determined in phyllosilicate and oxide phases by counting for 100 seconds on the element's peak and at two background positions. Beam conditions were 20 kV, 50 nA for trace element determinations (see also Ramsden and French, 1990).

The data from more than 600 major element arrays and approximately 500 trace element arrays were collected during the course of this study. As about 6 determinations were done for each mineral, these data were averaged for the more than 100 minerals discussed below.

3. RESULTS

3.1 White micas

Micas have the general formula $X_2\ Y_4\ (Si,Al)_8O_{20}(OH)_4$, where X = alkali and alkaline earth metals (e.g. Na, K, Ca) held in 12-fold coordination, Y = elements in octahedral coordination (e.g. Al, Fe), Si and some Al is in tetrahedral coordination. True micas have X site occupancies greater than 1.5 mols but illite and its Na analogue, brammallite, have a lower X-site occupancy. At Mt Magnet, micas and illites contain up to 1.24 mols Na and 0.87 mols Ca in the X sites (Table 1). Micas and illites from mafic volcanics are more likely to contain higher Na and/or Ca contents than their equivalents from felsic volcanics (Table 1).

In addition to their lower X-site occupancy, illite and brammallite are distinguished from their mica analogues, muscovite and paragonite, by a ΣY-site occupancy > 4.2 mols. Margarite has Si < 6 mols and high Al (>2.4 mols) in tetrahedral sites. F contents are generally low, with only sample (108344 from NMS D7) having F > 0.03 mols.

Fe* ratios (i.e. Fe/(Fe+Mg+Mn)) and Na contents tend to be higher in micas and illites from barren profiles than those from mineralized ones when material from similar lithologies are compared. Thus Na content is greater than 0.3 mols for barren mafic volcanics but lower in mineralized equivalent rocks. A smaller amount of data suggests that barren felsic volcanics have greater than 0.1 mols of Na (Fig. 2).

Cr contents tend to be greatest in the micas from ultramafic rocks (~1000 ppm) with intermediate values in those from mafic rocks (<100-870 ppm), with the lowest values (< 130 ppm) in the micas from felsic volcanics (Table 1). Ni is not present in micas and Cu and Zn generally < 200 ppm. Sr only occurs in paragonite or brammallite. Ba contents may be high (> 700 ppm) in mica or illite, especially those from highly mineralized profiles (i.e. NMS D4, NMS D7 and NMS D9). The illite from the ultramafic rock (108525) also has a high Ba content (~ 1000 ppm). Margarite from sample 105118 has a particularly low Ba content (Table 1).

3.2 Chlorite and Talc

Chlorite contains only octahedrally and tetrahedrally coordinated cations with Mg, Al and Fe in the octahedral sites and Si and Al in the tetrahedral sites. Talc also contains octahedrally and

tetrahedrally coordinated cations, but Mg totally dominates the octahedral (Y) sites and Si the tetrahedral sites.

Because chlorite weathers readily, it only occurs in relatively fresh material from mafic and felsic rocks at Mt Magnet. Thus the shallowest material analysed was from sample 105099 (NMS D4 : 58.3 m; true depth = 55m). However in ultramafic rocks, chlorite and talc are present at much higher levels in the profile, e.g. sample 108547 (PKN 039:27-28 m; true depth = 24 m).

Chlorite from ultramafic rocks tends to have lower Fe contents in octahedral sites and higher Si contents in tetrahedral sites than chlorites from mafic and felsic rocks (Table 2). Fe* ratios are lower and Mg contents higher for chlorite in mafic and felsic rocks associated with mineralization relative to that from unmineralized associations (Fig. 3). F contents are often ~0.4 mols i.e. considerably higher than in micas (cf. Tables 1 and 2).

Cr contents again reflect the host rocks with felsic-hosted chlorite having 170-300 ppm, mafic-hosted chlorite 260-650 ppm and ultramafic-hosted chlorite ~ 3000 ppm Cr. Ni contents < 500 ppm occur in the chlorites within mafic and felsic volcanics but Ni > 1000 ppm occurs in those of ultramafic rocks. Cu and Zn contents tend to be higher than in micas (Tables 1 and 2).

Talc has a lower Fe* ratio than co-existing chlorite and also tends to have low Cr but high Ni contents. These features readily distinguish it from chlorite (Table 2).

3.3 Kaolinite

Kaolinite has Si tetrahedrally coordinated and Al octahedrally coordinated, any impurities (especially Fe) are held in the octahedral sites. The dominance of the tetrahedral sites by Si thus means that considerable rearrangement of cations takes place during its formation from phyllosilicates during weathering.

Kaolinite is frequently contaminated by Fe oxides and/or illite as reflected by the presence of Fe and K in the analyses (Table 3). Minor element contents of the kaolinite also reflect lithologies with kaolinite from ultramafic rocks containing higher residual Cr than kaolinite from felsic or mafic rocks. However the base metal contents of the kaolinites are generally low (Table 3).

3.4 Tourmaline and feldspar

Tourmalines have the general formulae $XY_3\ Al_6\ B_3\ Si_6\ O_{27}(OH)_4$ where X = Na, K and Ca and Y = Fe, Mg and Al + Li. The B content cannot be analysed using the electron microprobe.

Tourmaline from mineralized mafic rocks within the pit area have Fe* $\leq$ 0.43, whereas the analysed tourmaline from outside the pit have higher Fe* values (Table 4). Although only three tourmaline-bearing samples were analysed, this feature of lower Fe contents associated with mineralization is consistent with the trend observed for micas and chlorites (Figs. 2 and 3).

Feldspars from 6 samples of mafic and felsic rocks from drill holes NMS D4, NMS D8 and NMS D9 vary in composition from An_1 to An_{16} i.e. albite to oligoclase.

3.5 Fe oxides and spinel

Hematite and goethite ideally should analyse at 100% and 90% Fe_2O_3 respectively. However, both Fe oxides occur as masses of very fine grained material and this feature, plus any additional found water in the Fe oxide structures, leads to lower than anticipated Fe_2O_3 contents (even after allowing for other components within the mineral structure or as included impurities). Nevertheless goethite is generally easily distinguished from hematite by its duller colour in back-scattered electron images (e.g. Fig. 4) and a grey rather than more yellow colour under reflected light (after carbon coating). Hematite components sum to > 90% but goethite components are generally < 85% (Table 5).

In goethite from samples 105111, 108525 and 108615, Al > Si implies that these samples are Al-goethites, some of the higher Si samples may also be Al-goethites and the Si due to submicroscopic quartz inclusions but this situation cannot be distinguished from goethite with small kaolinite inclusions using electron microprobe data.

Other features of the goethites are up to 3300 ppm As, 6500 ppm Cr, 1400 ppm Ni, 1.04% Cu, 240 ppm Mo, 5200 ppm Sb, 2700 ppm Zn, 530 ppm Co, 2.68% W and 1000 ppm V. SO_3 may be as high as 0.69% and P_2O_5 up to 0.90% (Table 5).

Residual goethite in veins tends to have higher base metal contents (As, Cu, Sb, Zn, V and W) than disseminated goethite (e.g. samples 105118 and 105130, Table 5). Al-goethite has higher SO_3, P_2O_5, As,

Cr, Ni, Cu but lower Sb and Zn than co-existing ordinary goethite from sample 105615 (Table 5).

Hematite contains up to 4000 ppm As, 3800 ppm Cr, 580 ppm Ni, 1800 ppm Cu, 560 ppm Sb, 230 ppm Zn, 0.38% SO_3 and 0.50% P_2O_5 (Table 5). Although maximum Cr, Ni, Cu, Sb, Zn, SO_3 and P_2O_5 contents are higher in goethite, comparison of coexisting goethite and hematite from samples 105097, 105099, 108369 and 108525 suggests that As and Ni are consistently higher in goethite and Zn and SO_3 in hematite. In many of these cases goethite rims hematite (e.g. Fig. 4).

Fe-Cr spinel in the ultramafic sample 108547 has high Cr, V and Zn contents with significant As, Cu, Sb and W also present (Table 5). The Fe-Mn oxide, jacobsite (ideally $MnFe_2O_4$, i.e. also a spinel group mineral; Roy, 1981) from the felsic sample 108369 is a primary mineral and occurs at a greater depth than the secondary Mn oxides (Section 3.7). It only contains significant amounts of Ni and Zn (Table 5).

3.6 Rutile

Rutile generally occurs as small < 10 µm grains, forming inclusions in micas and pyrite in fresh samples. However it is present as much larger grains ~ 50 x 100 µm in mafic and felsic rocks in NMS D7 at depths of 31 to 80 m (Table 6). It also occurs as > 100 µm grains in ultramafic rock at the base of PKN 039 (39-40 m; Table 6).

In felsic rocks it has Cr contents ranging from < 100 to 700 ppm, if the near surface sample 108323 in which Cr is substantially concentrated (Scott, 1989c) is disregarded. Rutile from mafic rocks has 120-1800 ppm Cr and that from ultramafic rocks 1000-1600 ppm Cr (Table 6). Average Cr contents are 360, 800 and 1300 ppm for rutiles from felsic, mafic and ultramafic rocks respectively.

3.7 Mn oxides

Secondary Mn oxide phases are well developed in the basal 15 m of ferruginous material in profiles at Mt Magnet (Scott 1989a, c), i.e. generally between 30 and 45 m (Table 7). Mn oxides rich in Na, K and Ba, having the general formula, $(Na, K, Ba)_{1-2}Mn_8O_{16}.\ x\ H_2O$, representing solid solution between manjiroite, cryptomelane and hollandite respectively, are found in the mafic and felsic volcanics at Mt Magnet (e.g. Fig. 5). These minerals may stabilize Co and Ni within their structures but even higher concentrations of these two elements are present in Al-rich lithiophorite ($(Al,Li)(OH)_2MnO_2$) from ultramafic rocks (Table 7).

3.8 Pyrite and other sulfides

Pyrite from mineralized profiles occurs in at least 3 generations which can be recognized chemically and texturally. The earliest (stage I) is Co- and/or Ni-rich and < 10 µm (best developed in sample 108348). Stage II pyrite is As-rich and may coat and/or replace stage I pyrite. It occurs as grains < 100 µm across. Stage III pyrite is As-poor and occurs as rims up to 30 µm thick about earlier pyrite grains or as grains up to 500 µm across and sometimes contains other sulfide phases, especially Cu sulfides and tetrahedrite (sample 108344; Table 8).

The Cu rich minerals chalcopyrite, chalcocite, covellite and tetrahedrite occur in samples 108344 and 108348 and contain variable amounts of Ag. In the former, tetrahedrite has the formula $(Cu_{9.5}Zn_{1.8}Fe_{1.3})(S_{13}Sb_{3.8}As_{0.2})$ and contains 800 ppm Ag. Chalcocite from the same sample contains <100 ppm Ag. In sample 108348 the tetrahedrite is more As- and Ag-rich but Zn and Sb poor as seen by its formula $(Cu_{9.1}Zn_{1.3}Fe_{1.1}Ag_{0.2})(S_{13}Sb_{3.4}As_{0.5})$. This Ag content is 1.1% by weight. Although chalcopyrite from that sample contains less than 100 ppm Ag, covellite contains 4100 ppm.

3.9 Carbonates

Dolomite is generally ferroan and has a Mn/Fe ratio ≤0.06, although the gold-rich sample 105099 (close to the base of oxidation in NMS D4) contains Fe-poor dolomite and has a much higher Mn/Fe ratio (0.41; Table 9). Siderite at Mt Magnet is quite Mn-rich. Calcite may also contain significant Mn, especially relative to low Fe contents (Table 9).

3.10 Gold

Gold is observed in sample 105073 and 105099 from NMS D4. In sample 105073 close to the surface, the gold occurs as (30 x 2 µm) stringers in Fe oxides (Fig 6) and (15 x 4 µm) blebs in voids (Fig 7). Such gold is secondary and contains no Ag. In sample 105099 close to the base of oxidation, gold occurs as Ag-bearing blebs up to 100 x 50 µm and as abundant grains in chlorite within a vein (Fig 8). The Ag content of such gold is 11.8 at %. One 50 µm grain of Ag-poor gold was also observed rimmed by the Ag-rich variety (Figs 9,10,11). As the Ag-rich variety appears to be primary, both types of Au of gold in this sample are probably primary. Thus it appears that secondary gold at Mt Magnet loses the Ag-content which is generally associated with primary gold.

4. DISCUSSION

4.1 Mineralogical changes during weathering

Unweathered mafic and felsic assemblages at Mt Magnet consist of quartz, sodic plagioclase, mica, chlorite, carbonate and sulfides (Scott 1989a,c). Ultramafic profiles have not been completely sampled at Mt Magnet but would be expected to consist of assemblages of quartz, carbonate, chlorite and talc as found at Panglo (Scott 1990a). Minor to trace amounts of rutile, spinel, tourmaline and gold are also present in the various rocks at Mt Magnet (as seen above). A 10 x 1 μm needle of thortveitite ($Sc_2Si_2O_7$) - a mineral usually found associated with pegmatites was found associated with an Fe oxide/kaolinite vein in one sample of weathered mafic volcanics (sample 105118; NMS D5: 53.2 m). These minerals can be considered in 3 groups according to their stability during weathering (a) resistant (quartz, tourmaline, spinel, rutile and mica), (b) partially resistant (gold and talc) and (c) unstable (sulfides, chlorite, feldspars and carbonates). New mineral species (Fe oxides, Mn oxides, kaolinite and smectites) generated by weathering of the third group, form an additional group. The effects upon whole-rock chemistry caused by weathering of each of these minerals (except quartz and thortveitite) is considered below.

4.1.1 Resistant minerals

Tourmaline provides a host for Na and Mg and spinels a host for Mn, Cr, Ni, Zn and V (Tables 4 and 5). However neither of these minerals is particularly abundant so that their effect in stabilizing Na, Mg, Mn, Ni and Zn (which are often quite mobile during weathering) is usually minimal.

Rutile is generally resistant to weathering, effectively stabilizing its usually significant Cr content (Table 6). Although in extremely weathered material close to the surface, it does appear to have incorporated additional Cr, it is useful as a lithological indicator (Section 4.3).

Micas generally persist through the weathered zone at Mt Magnet although they are sometimes degraded to illite-brammallite. Such "white micas" are the major host mineral for K and Ba (Table 1). Na and Sr, which are normally mobile during weathering, may be retained in paragonite and brammallite. Up to 1200 ppm Cr may also be stabilized in mica (Table 1; Section 3.1).

4.1.2 Partially resistant minerals

Gold occurs mainly as Ag-rich grains (11.8 at % Ag; Section 3.10) in unweathered rock but during weathering it loses its Ag content as generally found elsewhere in the Murchison Goldfields (e.g. Freyssinet and Butt, 1988). Because whole rock analyses indicate that Ag may maintain its association with Au in the weathered profile at Mt Magnet (Scott 1989a), such Ag is probably incorporated into Fe oxides with other elements like As (Section 3.5).

Talc is only significant in ultramafic profiles in which it persists to about half way up the weathered zone at Mt Magnet (Scott 1990b). Thus it retains Mg and Ni well after minerals like feldspar and carbonates have been destroyed.

4.1.3 Unstable minerals

These minerals are generally completely weathered at vertical depths of 50-60 m at Mt Magnet (e.g. Scott 1989a,c).

Pyrite occurs as at least 3 types - an early <10 µm Co-bearing phase, a larger As-rich phase and a late As-poor phase which frequently rims the earlier phases. This late phase may also contain inclusions of other sulfides (Section 3.8). These features and the general association of As with Au in weathered material at Mt Magnet (Scott 1989a,c) are consistent with the second (or As-rich) pyrite phase being most directly associated with the gold. The As, Co, Cu, Ni, Sb and Zn which occur in the pyrites (Table 8) are all incorporated, to some extent, in Fe oxides during weathering (Table 5).

Tetrahedrite bears substantial (800 ppm - 1.1%) Ag but the other primary Cu-rich sulfides chalcopyrite and chalcocite contain <100 ppm Ag (Section 3.8). The ?secondary covellite contains ~4000 ppm Ag. All this Ag, in addition to that originally associated with primary gold, is mobilized during weathering although as seen above (Section 4.1.2) some of it is probably incorporated into Fe oxides.

Chlorite is a major host for Fe, Mg, Cr, Cu, Ni and Zn in rocks at Mt Magnet but it is readily weathered, except in ultramafic sequences where it may persist to within 24 m of the surface (Scott 1990b). Its component elements are generally lost (e.g. Mg) or incorporated, at least partially, into Fe oxides and kaolinite e.g. Cr (Section 3.3).

Plagioclase feldspar, albite or oligoclase, is completely weathered out of the profile above 50 m in the Parkinson Pit (e.g. NMS D7; Scott 1989b). However 300 m to the west of the pit it persists to within 13 m of the surface in PKN 049 (Scott, 1990b). Its Na and Ca contents are essentially lost during weathering (they may be partially retained in smectitic clays; Section 4.1.4). Although not analysed during this study minor Sr and Ba probably also occur in these plagioclase feldspars, as at Panglo (Scott, unpublished data).

Carbonates readily weather to Fe and Mn oxides with the other major components being readily dispersed during weathering. As in the feldspars, trace amounts of Sr and Ba probably occur in the carbonates, especially calcite and dolomite (Scott, unpublished data), and these elements may be directly incorporated into the Mn oxides (Table 7) which form over the 15 m directly above weathering carbonates (Section 3.7).

4.1.4 Weathering products

Fe oxides form from material derived from chlorite, carbonates and sulfides. When derived from sulfides they appear to contain significant chalcophile element contents especially As, Cu, Sb, Zn and W (Section 3.5; Table 5). Similar concentration of chalcophile elements in goethite formed from sulfides is observed at Callion (Llorca, 1989). Cr and V may also be substantially concentrated in Fe oxides, probably reflecting material derived from chlorite (cf. Table 2).

Mn oxides occur in the 15 m above the base of oxidation at Mt Magnet and are probably derived from weathering carbonates as suggested by the open texture of the cryptomelane in NMS D8 (Fig 5) and the high Mn content of the carbonates (Section 3.9). The Mn oxide phases stabilize Co and Ni (derived from pyrite and chlorite) and Ba and Sr (derived from feldspars, carbonates and possibly from a small amount of mica). Similar Mn oxides occur toward the base of the weathering profile through mafic volcanics at Beasley Creek, near Laverton (Robertson and Gall, 1988) and at a similar or somewhat higher level at Panglo (Scott, 1990a).

Kaolinite is an abundant weathering product at Mt Magnet. Although it may contain some Cr when derived by the weathering of a high Cr mineral like chlorite, as also seen at Panglo (Scott, 1989b; Section 3.3), its base metal content is generally low, especially relative to co-existing goethite (cf. Samples 108546 and 108559; Tables 3 and 5). Such low base metal contents reflect the loss of the octahedrally

coordinated cations as structural re-arrangements take place to form kaolinite from say, chlorite (Section 3.3).

Smectitic clays occur in trace to minor amounts through the weathered profiles at Mt Magnet (e.g. Scott 1989c). However, because they were never found during electron microprobe study, they must occur as very small (<5 μm) grains and/or be admixed with other phases. They may be responsible for stabilizing small amounts of Na and Ca (cf. Llorca, 1989).

4.2 Mineralogical features reflecting mineralization

Micas at Mt Magnet generally survive weathering although in some cases they may degrade to illite-brammallite. Such degradation involving the loss of K from the large ion (X) sites does not markedly affect octahedrally coordinated ions (in Y sites). Hence the Fe* ratio is retained during weathering and thus "white micas" with Fe* <0.7 give some indication of proximity to mineralization. Similarly the low Na contents of such "white micas" appears to indicate proximity to mineralization (Section 3.1, Fig 2).

This tendency to lower Fe contents in micas also appears to be developed in chlorite and tourmaline (Sections 3.2, 3.4). Such parallel behaviour has previously been noted in a wide range of unweathered rocks about various types of deposits e.g. porphyry Cu and disseminated Sn deposits (Scott, 1978; 1988) and massive sulfide deposits (McLeod, 1987; Slack and Coad, 1989). Conversely high Fe contents and/or low Mn/Fe ratios in dolomites suggest proximity to mineralization e.g. stratiform Pb-Zn deposits (Lambert and Scott, 1973), epigenetic Cu deposits (Scott, 1989d) and Archaean gold deposits (Groves and Phillips, 1987). Although the few analysed dolomites from mineralized drill holes at Mt Magnet generally have Mn/Fe ≤0.06, sample 105099 has a higher ratio (Table 9) possibly due to secondary carbonate formation at the base of oxidation. Because chlorite and dolomite are generally unstable to weathering and tourmaline is not present in every sample from Mt Magnet, the "white micas" offer the best lithogeochemical guide to mineralization in weathered material.

4.3 Mineralogical features reflecting lithology

The Cr content of micas, chlorites and rutiles broadly reflect rock types at Mt Magnet. Thus micas derived from ultramafic rocks contain ~1200 ppm Cr, those from mafic rocks <100-870 ppm Cr and those from felsic rocks <130 ppm Cr. The Na and/or Ca contents of micas of mafic

rocks may also be higher than in the micas of the felsic rocks (Table 1, Section 3.1).

The Cr content of chlorites decreases from ~3000 ppm Cr in ultramafic rocks to 260-650 ppm for mafic rocks to ~170 ppm for felsic rocks (with Ni contents also showing a similar decrease as rocks become more felsic, Table 2).

Rutile has Cr contents of 1000-1600 ppm in ultramafic rocks, 120-1800 in mafic rocks and <100-700 ppm in felsic rocks (Table 6; Section 3.6). The high Cr content in spinel from ultramafic sample (108547, Table 5) and its absence from the spinel in a felsic rock (108369) is also consistent with this trend of decreasing Cr as the rocks become more felsic. Scott (1989b) also suggested that goethite may show this trend in mafic and ultramafic profiles at Panglo, but it is only poorly developed (if at all) at Mt Magnet (Table 5).

Thus in weathered rocks at Mt Magnet, the Cr content of micas and rutile presents the best mineralogical information about lithology.

5. CONCLUSIONS

Minerals in fresh and weathered samples at Mt Magnet can be divided into four groups, on the basis of their weathering properties - resistant, partially resistant, unstable and new-formed weathering products. The resistant group consists of quartz, rutile, tourmaline, mica and spinel with the decreasing Fe content of tourmaline and mica appearing to be an indicator of proximity to mineralization. Talc and gold make up the partially resistant group with talc reflecting ultramafic rocks to a much higher level in the profile than chlorite. The loss of Ag from gold during weathering reflects secondary gold formation during weathering at Mt Magnet. Sulfides, chlorite, feldspars and carbonates do not generally survive long after the commencement of weathering but where present, chlorite, and perhaps carbonate, compositions may reflect proximity to mineralization. The compositions of sulfides, especially As-rich pyrite, also are related to mineralization. Fe oxides, Mn oxides, kaolinite and smectitic clay are all formed during weathering with the Fe oxides hosting substantial amounts of the Au-pathfinder elements e.g. As, Sb and W. Mn oxides are important hosts to Co, Ni, Ba and Sr at the base of the weathered profile.

Lithological associations are reflected by decreasing Cr contents of rutile, mica, chlorite and perhaps spinel as rocks change from ultramafic to mafic to felsic.

6. RECOMMENDATION

The small amount of data on pyrite and carbonate compositions presented in this report suggest that further study of fresh material (although outside the scope of AMIRA Project 241) may be worthwhile in ongoing exploration for primary gold mineralization at Mt Magnet.

7. ACKNOWLEDGEMENTS

The past and present geological staff of Metana Minerals NL at Mt Magnet (Steve Hunt, David Bartlett, Alan Wilson, David Bright and John Everard) are thanked for logistic help and discussions.

Samples were prepared for electron microprobe analysis by Manal Kassis. Assistance with electron microprobe operations and photography was provided by David French and Ken Kinealy (all of the North Ryde laboratories of the CSIRO, Division of Exploration Geoscience).

8. REFERENCES

Freyssinet, Ph. and Butt, C.R.M., 1988. Morphology and geochemistry of gold in a lateritic profile, Reedy Mine, Western Australia (AMIRA P241: Weathering Processes) CSIRO Div. of Exploration Geoscience Restricted Report MG 58R.

Groves, D.I. and Phillips, G.N., 1987. The genesis and tectonic control on Archaean gold deposits of the Western Australian Shield - a metamorphic replacement model. Ore Geology Reviews 2: 287-322.

Lambert, I.B. and Scott, K.M., 1973. Implications of geochemical investigations of sedimentary rocks within and around the McArthur zinc-lead-silver deposit, Northern Territory. J. Geochem. Explor. 2: 307-330.

Llorca, S.M., 1989. Mineralogy and geochemistry of the Glasson Gold Deposit, Callion, Yilgarn Block, W.A. (AMIRA P241: Weathering Processes) CSIRO Div. of Exploration Geoscience Restricted Report 58R.

McLeod, R.L., 1987. Alteration associated with volcanogenic sulphide ores at Mount Chalmers, Queensland. Trans. Inst. Min. Metall. (Sect. B: Appl. Ea. Sci) 96: 117-127.

Ramsden, A.R. and French, D.H., 1990. Routine trace-element capabilities of electron microprobe analysis in mineralogical investigations : an empirical evaluation of performance using spectrochemical standard glasses. Can. Mineralogist 28 : 171-180.

Roy, S., 1981. Manganese Deposits. Academic Press, London. 458pp.

Robertson, I.D.M. and Gall, S.F., 1988. A mineralogical, geochemical and petrographic study of the rocks of drillhole BCD1 from the Beasley Creek Gold Mine - Laverton, W.A. (AMIRA P241: Weathering Processes) CSIRO Div. of Exploration Geoscience Restricted Report MG 67R.

Scott, K.M., 1978. Geochemical aspects of the alteration-mineralization at Cooper Hill, New South Wales, Australia. Econ. Geol. 73: 966-976.

Scott, K.M., 1988. Phyllosilicate and rutile compositions as indicators of Sn specialization in some southeastern Australian granites. Mineral. Deposita 23: 159-165.

Scott, K.M., 1989a. Mineralogy and geochemistry of mineralized and barren weathered profiles, Parkinson Pit, Mt Magnet, W.A. (AMIRA P421: Weathering Processes) CSIRO Div. of Exploration Geoscience Restricted Report 33R.

Scott, K.M., 1989b. Mineralogy and geochemistry of weathered mafic/ultramafic volcanics from Section 4200N at Panglo, Eastern Goldfields, W.A. (AMIRA P241: Weathering Processes) CSIRO Div. of Exploration Geoscience Restricted Report 42R.

Scott, K.M., 1989c. Mineralogy and geochemistry of mineralized and barren felsic volcanic profiles, Parkinson Pit, Mt Magnet, W.A. (AMIRA P241: Weathering Processes) CSIRO Div. of Exploration Geoscience Restricted Report 73R.

Scott, K.M., 1989d. Dolomite compositions as a guide to copper mineralization, Mount Isa Inlier, NW Queensland. Mineral. Deposita 24: 29-33.

Scott, K.M., 1990a. The mineralogical and geochemical effects of weathering on volcanics from the Panglo Deposit, Eastern Goldfields, W.A. (AMIRA P241: Weathering Processes) CSIRO Div. of Exploration Geoscience Restricted Report 143R.

Scott, K.M., 1990b. The mineralogical and geochemical effects of weathering in mafic and ultramafic profiles, Mt Magnet, W.A. (AMIRA P241: Weathering Processes) CSIRO Div. of Exploration Geoscience Restricted Report (in prep.).

Slack, J.F. and Coad, P.R., 1989. Multiple hydrothermal and metamorphic events in the Kidd Creek volcanogenic massive sulphide deposit, Timmins, Ontario: evidence from tourmaline and chlorites. Can. J. Earth Sci. 26: 694-715.

Table 1. Structural formulae (based on 22 0) and trace element contents for white micas, Mt Magnet

Sample No.	105094	105097	105099	105103	105111	105111	105118	105118	105122	108325	108331
Drill hole	NMS D4	NMS D4	NMS D4	NMS D4	NMS D5	NMS D5	NMS D5	NMS D5	NMS D5	NMS D7	NMS D7
Depth (m)	46.7	52.0	58.3	70.8	31.9	31.9	53.2	53.2	68.0	10.5	31.2
No. of analyses	7	6	5	6	7	4	4	6	7	8	7
K	0.94	1.46	1.04	0.92	0.22	0.22	0.27	0.45	1.41	0.92	1.35
Na	0.26	0.18	0.21	0.67	1.22	0.81	0.63	0.58	0.32	0.08	0.08
Ca	0	0	0	0.01	0.08	0.08	0.87	0.66	0.02	0	0[1]
ΣX	1.20	1.64	1.25	1.60	1.52	1.11	1.77	1.69	1.75	1.00	1.44
Al	3.98	3.80	4.01	3.86	4.03	4.16	3.94	3.96	3.90	4.04	3.89
Fe^{II}	0.21	0.13	0.10	0.11	0.04	0.04	0.06	0.07	0.06	0.09	0.14
Mg	0.08	0.12	0.07	0.05	0.01	0.01	0.02	0.03	0.03	0.11	0.15
Mn	0.01	0	0	0.01	0	0	0	0	0	0	0
Ti	0	0.01	0.01	0.01	0	0	0.01	0	0.01	0.01	0
Cr	0	0	0.01	0.01	0.01	0.01	0.01	0.01	0.01	0	0
ΣY	4.28	4.06	4.20	4.05	4.09	4.22	4.04	4.07	4.01	4.25	4.18
Si	6.25	6.39	6.33	6.40	6.18	6.23	5.30	5.54	6.28	6.41	6.28
Al	1.75	1.61	1.67	1.60	1.82	1.77	2.70	2.46	1.72	1.59	1.72
OH	3.97	3.93	3.98	3.98	3.99	4.02	3.95	3.97	3.97	3.95	3.94
F	0.01	0.03	0.03	0	0.01	0.01	0.03	0.02	0.03	0.01	0.03
Cl	0.01	0.01	-	0.02	-	-	0.01	0.01	0	0.01	0.01
Cr (ppm)	<100	330	870	400	470	480	500	540	430	120	<100
Ni (ppm)	<100	<100	<100	<100	<100	<100	<100	<100	<100	<100	<100
Cu (ppm)	130	220	<100	<100	120	<100	280	240	<100	<100	100
Zn (ppm)	<100	<100	<100	<100	120	100	<100	<100	<100	<100	<100
Sr (ppm)	<100	<100	<100	<100	390	-	<100	<100	<100	<100	<100
Ba (ppm)	450	260	720	300	380	-	<100	<100	310	260	1500
Fe*	0.72	0.53	0.57	0.52	0.79	0.79	0.77	0.71	0.68	0.46	0.49
Mineral	Illite	Musc	Illite	Na-musc	Para	Bram.	Margarite		Na-musc	Illite	Illite
Rock type	← mafic →									← felsic →	

Note [1]0.01 Ba also present
Musc ≡ muscovite, Para ≡ Paragonite, Bram ≡ Brammallite

Table 1 (continued)

Sample No.	108334	108334	108344	108348	108366	108369	108371	105144	108525	108615	108615	108630	108630
Drill hole	NMS D7	NMS D7	NMS D7	NMS D7	NMS D8	NMS D8	NMS D8	NMS D9	PKN 039	PKN 203	PKN 203	PKN 203	PKN 203
Depth (m)	44.2	44.2	79.9	103.8	44.9	56.6	62.0	73.6	5-6	15-16	15-16	30-31	30-31
No. of analyses	7	4	6	6	6	4	6	7	8	8	4	4	3
K	1.59	1.04	1.78	1.60	1.24	1.43	1.75	1.73	1.11	1.20	0.34	1.35	0.39
Na	0.05	0.05	0.09	0.12	0.15	0.14	0.17	0.16	0.09	0.32	0.74	0.38	1.24
Ca	0	0	0	0.01	0	0	0[1]	0.02[1]	0[1]	0[1]	0.01	0	0.01
ΣX	1.64	1.09	1.87	1.73	1.39	1.57	1.93	1.92	1.21	1.53	1.09	1.73	1.64
Al	3.78	4.04	3.74	3.57	3.89	3.84	3.81	3.68	3.62	3.82	4.08	3.80	3.92
Fe^{II}	0.16	0.15	0.10	0.36	0.29	0.15	0.12	0.23	0.54	0.34	0.16	0.28	0.23
Mg	0.18	0.10	0.18	0.23	0.07	0.10	0.09	0.11	0.17	0.04	0.01	0.06	0.03
Mn	0	0	0	0	0	0	0	0	0	0	0	0	0
Ti	0.02	0.01	0.02	0.02	0.01	0.02	0.01	0.01	0.01	0	0	0	0
Cr	0.01	0.01	0	0.01	0	0	0	0.01	0.01	0.01	0	0	0
ΣY	4.15	4.31	4.04	4.19	4.26	4.11	4.03	4.04	4.35	4.21	4.25	4.14	4.18
Si	6.23	6.23	6.28	6.29	6.16	6.32	6.13	6.26	6.40	6.18	6.28	6.12	6.09
Al	1.77	1.77	1.72	1.71	1.84	1.68	1.87	1.74	1.60	1.82	1.72	1.88	1.91
OH	3.97	3.99	3.97	4.02	3.96	3.97	3.93	3.98	3.95	3.94	3.94	3.92	4.00
F	0.03	0.02	0.04	0.01	0.02	0.02	0.03	0.02	0.01	0.03	0.02	0.01	0.02
Cl	0	0	0	0	0	0	0	0	0.01	0	0	0	0
Cr (ppm)	680	450	<100	420	130	120	<100	410	1200	420	300	170	180
Ni (ppm)	<100	<100	<100	<100	<100	<100	<100	<100	<100	<100	<100	<100	<100
Cu (ppm)	<100	<100	<100	100	<100	<100	<100	290	170	<100	140	<100	<100
Zn (ppm)	<100	<100	<100	<100	<100	<100	<100	170	<100	<100	<100	<100	<100
Sr (ppm)	<100	<100	<100	<100	<100	<100	<100	<100	<100	<100	190	<100	220
Ba (ppm)	630	290	650	180	300	290	1300	1800	1000	910	380	650	240
Fe*	0.46	0.58	0.35	0.60	0.80	0.60	0.56	0.67	0.76	0.88	0.94	0.82	0.89
Mineral	Musc	Illite	Musc	Musc	Illite	Musc	Musc	Musc	Illite	Na-musc	Bram	Na-musc	Para
Rock type	← mafic →		felsic	mafic	← felsic →			mafic	ultramafic	← mafic →			

Note [1]0.01 Ba also present

Table 2. Structural formulae (based on 28 0 and 22 0 respectively) and trace element contents for chlorite and talc, Mt Magnet

Sample No.	105099	105103	105118	105122	108344	108348	108731	105144	108547	108547	108559
Drill hole	NMS D4	NMS D4	NMS D5	NMS D5	NMS D7	NMS D7	NMS D8	NMS D9	PKN 039	PKN 039	PKN 039
Depth (m)	58.3	70.8	53.2	68.0	79.9	103.8	62.0	73.6	17-18	17-18	39-40
No. of analyses	8	6	6	6	6	6	4	6	6	4	8
	Chlorite									Talc	Chl
Mg	5.02	3.64	3.42	3.34	5.08	4.82	3.76	3.82	5.51	5.11	4.33
Al	3.26	3.18	3.83	3.62	3.15	2.81	3.48	3.17	3.16	0.03	3.65
Fe^{II}	3.22	4.65	3.75	4.35	3.29	4.20	3.62	4.56	2.10	0.86	2.86
Mn	0.01	0.01	0.01	0.01	0.01	0.01	0	0.01	0	0.01	0.01
K	0.01	0.23	0.05	0.11	0.10	0.01	0	0.02	0.07	0	0.12
Na	0.01	0.04	0.10	0.04	0.01	0.02	0.02	0.03	0.03	0	0.03
Ca	0.01	0	0.12	0.01	0	0.03	0.01	0.03	0.04	0	0.02
Ti	0.01	0.01	0.01	0.04	0.01	0.02	0.01	0.01	0	0	0.01
Cr	0.02[1]	0.01	0.02[2]	0.01	0.01[3]	0.01[3]	0.01[1]	0.02[4]	0.09[5]	0[6]	0.05[7]
ΣY	11.59	11.77	11.33	11.53	11.67	11.94	10.93	11.72	11.10	6.03	11.12
Si	5.60	5.52	5.62	5.35	5.63	5.31	6.64	5.43	6.58	7.98	6.25
Al	2.40	2.48	2.39	2.65	2.37	2.69	1.36	2.57	1.42	0	1.75
OH	15.96	15.93	15.94	15.96	15.98	15.99	15.94	16.00	15.95	4.00	15.99
F	0.04	0.05	0.04	0.01	0.05	0.02	0.05	0.03	0	0.01	0.04
Cl	-	0.02	0.02	0	0.01	0.01	0	0	0.01	0	0
Cr (ppm)	570	260	650	560	170	500	300	600	3600	<100	3100
Ni (ppm)	430	<100	<100	<100	<100	<100	360	700	2800	1200	1000
Cu (ppm)	<100	110	360	<100	100	130	<100	310	370	180	260
Zn (ppm)	630	<100	420	<100	250	320	390	890	1300	270	340
Fe*	0.39	0.56	0.52	0.57	0.39	0.47	0.49	0.54	0.28	0.15	0.40
Rock type	← mafic →				felsic	mafic	felsic	mafic	← ultramafic →		

Note: [1] Ni = 0.01, Zn = 0.01; [2] Cu = 0.01, Zn = 0.01; [3] Zn = 0.01; [4] Ni = 0.01, Zn = 0.01, Cu = 0.01
[5] Ni = 0.06, Zn = 0.03, V = 0.01; [6] Ni = 0.02; [7] Ni = 0.02, Cu = 0.01, Zn = 0.01 also present.

Table 3. Structural formulae (based on 14 0) and trace element contents for kaolinite, Mt Magnet

Sample No.	108323	108325	108334	108366	108369	108547	108559
Drill hole	NMS D7	NMS D7	NMS D7	NMS D8	NMS D8	PKN 039	PKN 039
Depth (m)	3.3	10.5	44.2	44.9	56.6	27-28	39-40
No. of analyses	5	4	2	6	3	4	4
Al	3.64	3.73	3.88	3.81	3.75	3.69	3.56
Fe^{III}	0.07	0.03	0.05	0.15	0.05	0.23	0.33
Si	0.19	0.10	0.02	0	0.04	0	0
Mg	0.02	0.03	0.02	0.01	0.03	0.14	0.30
Na	0.02	0.05	0.01	0.02	0.04	0.01	0.01
Ca	0.01	0	0	0.01	0.01	0.01	0.01
K	0.01	0.22	0.09	0.11	0.34	0	0.01[1]
ΣY	3.96	4.16	4.07	4.11	4.26	4.08	4.23
Si	4.00	4.00	4.00	3.98	4.00	3.98	3.92
OH	7.97	7.98	7.97	7.96	8.01	7.99	8.01
F	0.01	0.01	0.01	0.01	0.01	0	0.01
Cl	0	0.02	0	0	0	0	0
Cr (ppm)	250	150	160	130	<100	240	620
Cu (ppm)	160	<100	<100	<100	<100	<100	<100
Zn (ppm)	<100	<100	<100	<100	<100	100	100
Ba (ppm)	<100	<100	160	140	250	<100	<100
Rock type	← felsic →		mafic	← felsic →		ultramafic	

Note[1] Cr = 0.01 also present
All Ni and Sr contents <100 ppm

Table 4. Structural formulae for tourmaline (based on 16 0)[1], Mt Magnet

Sample No.	108334	108378	108378	108615
Drill hole	NMS D7	Pit	Pit	PKN 203
depth (m)	44.2	40	40	15-16
No. of analyses	3	5	4	3
Na	0.72	0.50	0.57	0.64
K	0.01	0	0	0
Ca	0.01	0.02	0.05	0.03
ΣX	0.74	0.52	0.62	0.67
Mg	1.92	1.52	1.44	1.34
Fe^{II}	0.85	0.97	1.08	1.66
Al	0.36	0.73	0.64	0.30
Ti	0.03	0.01	0.05	0.02
Cr	0.01	-	-	0
ΣY	3.17	3.23	3.21	3.32
Si	6.07	6.24	6.16	5.99
Al	6.00	6.00	6.00	6.00
Fe*	0.31	0.39	0.43	0.55
Type	Dravite	Dravite	Dravite	Schorl

Note [1] B content assumed to be 3 mols

Table 5. Compositions of Fe oxides and spinels (wt%), Mt Magnet

Sample No.	105073	105094	105097	105097	105099	105099	105111
Drill hole	NMS D4	NMS D4	NMS D4	NMS D4	NMS D4	NMS D4	NMS D5
Depth (m)	4.1	46.7	52.0	52.0	58.3	58.3	31.9
No. of analyses	7	6	6	5	8	3	5
Mineral	Goe	Hem	Goe	Hem	Goe	Hem	Al-goe
Fe_2O_3	59.9	84.6	80.2	86.8	74.1	85.7	68.6
TiO_2	-	<0.1	<0.1	<0.1	<0.1	<0.1	0.37
MnO	-	1.80	0.15	0.76	0.14	0.16	<0.05
Al_2O_3	2.98	0.61	0.31	0.46	2.09	0.39	13.1
SiO_2	4.03	3.08	3.24	3.05	4.26	2.78	7.11
SO_3	0.24	<0.1	0.11	0.21	<0.1	<0.1	0.15
P_2O_5	<0.1	0.12	<0.1	<0.1	0.26	0.11	0.61
As (ppm)	3300	<100	1300	890	<100	<100	630
Cr (ppm)	1100	<100	<100	<100	<100	<100	2100
Ni (ppm)	-	-	1400	580	-	-	820
Cu (ppm)	2400	-	580	530	-	-	3200
Mo (ppm)	240	-	-	-	-	-	-
Sb (ppm)	5200	-	<100	180	-	-	1300
Zn (ppm)	-	-	120	180	-	-	250
Rock type	← mafic →						

Sample No.	105118	105118	108331	108334	108369	108369	108369
Drill hole	NMS D5	NMS D7	NMS D7	NMS D7	NMS D8	NMS D8	NMS D8
Depth (m)	53.2	53.2	31.2	44.2	56.6	56.6	56.6
No. of analyses	4	4	6	7	5	6	6
Mineral	Goe (vein)	Goe (diss)	Hem	Goe	Goe	Hem	Jacob-site
Fe_2O_3	72.2	71.5	85.8	75.3	76.7	87.5	56.1
TiO_2	<0.1	<0.1	<0.1	0.43	<0.1	<0.1	<0.1
MnO	2.08	4.18	<0.05	0.99	0.16	0.06	21.4
Al_2O_3	2.75	1.54	0.59	1.61	1.25	0.43	1.50
SiO_2	3.82	4.16	1.44	3.05	4.48	3.10	2.11
SO_3	<0.1	<0.1	0.38	0.20	<0.1	0.30	0.16
P_2O_5	<0.1	0.10	0.46	0.31	0.13	0.50	0.17
As (ppm)	1500	200	4000	330	<100	270	<100
Cr (ppm)	390	<100	590	170	<100	<100	<100
Ni (ppm)	760	320	150	-	-	-	430
Cu (ppm)	1.04%	2200	1800	-	-	-	170
Mo (ppm)	-	-	-	-	-	-	-
Sb (ppm)	3200	1000	560	-	-	-	-
Zn (ppm)	2700	1600	190	-	-	-	830
Rock type	← mafic →		felsic	mafic	← felsic →		

Table 5 (continued)

Sample No.	108525	108325	108547	108547	108547	108559	108615	108615	108630	108630
Drill hole	PKN 039	PKN039	PKN039	PKN039	PKN039	PKN039	PKN203	PKN203	PKN203	PKN203
Depth (m)	5-6	5-6	27-28	27-28	27-28	39-40	15-16	15-16	30-31	30-31
No. of analyses	5	1	7	4	2	6	3	5	9	6
Mineral	Al-goe	Hem	Goe	Spinel	Spinel	Goe	Al-goe	Goe	Geo (vein)	Goe (diss)
Fe_2O_3	72.0	81.4	74.8	90.6	79.4	78.1	80.3	78.1	73.2	79.0
TiO_2	<0.1	<0.1	<0.1	<0.1	<0.1	0.16	<0.1	<0.1	<0.1	<0.1
MnO	0.06	<0.05	1.00	<0.05	0.07	0.24	<0.05	0.05	0.08	0.05
Al_2O_3	7.62	3.07	1.76	0.16	0.32	1.14	4.50	1.72	0.93	0.48
SiO_2	4.17	5.04	3.70	0.30	0.11	3.14	0.97	2.69	3.52	3.03
SO_3	0.17	0.15	<0.1	<0.1	0.11	0.10	0.69	0.35	<0.1	<0.1
P_2O_5	0.18	0.18	0.21	<0.1	<0.1	0.32	0.90	0.56	0.20	0.31
As (ppm)	580	130	110	180	140	1300	300	<100	570	280
Cr (ppm)	4100	3800	1500	4.24%	11.3%	840	6500	2000	250	240
Ni (ppm)	270	<100	730	330	480	630	370	250	160	260
Cu (ppm)	610	320	650	170	100	6600	1800	960	1500	810
Mo (ppm)	-	-	-	-	-	-	-	-	-	-
Sb (ppm)	110	<100	120	<100	170	430	<100	170	130	110
Zn (ppm)	100	230	890	9200	5200	110	260	390	720	660
Co (ppm)	-	-	530	150	<100	<100	-	-	220	320
W (ppm)	-	-	260	120	<100	<100	-	-	2.68%	400
V (ppm)	-	-	450	1400	1600	700	-	-	1000	<100
Rock type	← ultramafic →						← mafic →			

Table 6. Compositions of rutiles (wt%), Mt Magnet

Sample No.	105099	105103	105111	105122	108323	108325	108331	108334	108344	108348	108366	108371	105144	108525	108559
Drill hole	NMS D4	NMS D4	NMS D5	NMS D5	NMS D7	NMS D7	NMS D7	NMS D7	NMS D7	NMS D7	NMS D8	NMS D8	NMS D9	PKN039	PKN039
Depth (m)	58.3	70.8	31.9	68.0	3.3	10.5	31.2	44.2	79.9	103.8	44.9	62.0	73.6	5-6	39-40
No. of analyses	6	4	5	7	5	7	6	4	7	6	6	7	7	2	3
TiO_2	95.0	89.4	95.2	94.0	94.8	95.4	98.1	98.2	98.0	91.8	96.3	94.3	95.0	88.6	96.8
Fe_2O_3	0.92	1.80	0.89	0.21	0.21	0.28	0.27	0.21	0.26	0.62	0.50	0.39	0.73	3.07	0.44
MnO	<0.05	0.05	<0.05	<0.05	<0.05	<0.05	<0.05	<0.05	<0.05	<0.05	<0.05	<0.05	<0.05	<0.05	<0.05
Al_2O_3	0.23	1.03	0.20	0.79	0.22	0.19	<0.1	<0.1	0.19	1.85	0.16	1.27	0.28	0.30	<0.1
SiO_2	0.89	4.34	1.17	0.84	1.06	0.38	0.12	<0.1	0.30	2.68	0.66	1.55	0.64	4.84	0.52
Cr (ppm)	640	440	1300	3300	1200	300	700	120	<100	1500	<100	680	1800	1600	1000
Ni (ppm)	<100	-	270	-	-	-	-	-	-	-	-	-	-	-	-
Rock type	← mafic →				← felsic →			mafic	felsic	mafic	← felsic →		mafic	ultramafic	
Grain size	← ~5 x 10 µm →				← 50x100 µm →					← ~5x10 µ →					>100 µm

Table 7. Compositions of Mn oxides (wt%), Mt Magnet

Sample No.	105094	105118	108366	108559
Drill hole	NMS D4	NMS D5	NMS D8	PKN 039
Depth (m)	46.7	53.2	44.9	39-40
No. of analyses	4	5	4	6
Mineral	Cryptomelane	Manjiroite	Cryptomelane	Lithiophorite
MnO_2	68.2	71.5	76.8	58.2
Fe_2O_3	3.07	4.43	2.60	3.55
Al_2O_3	2.18	0.45	0.64	9.76
Na_2O	0.59	1.08	0.60	0.37
K_2O	2.46	0.76	3.27	0.45
BaO	0.16	1.39	0.72	1.15
SrO	0.19	0.06	0.38	0.07
CaO	0.40	0.67	0.70	0.46
PbO	0.01	0.04	0.08	<0.01
CuO	0.10	0.09	0.03	0.14
ZnO	0.12	0.08	0.08	0.02
CoO	1.12	0.37	0.11	1.30
NiO	0.40	0.10	0.07	2.14
V_2O_5	0.04	-	0.01	0.14
Sb_2O_5	-	0.01	-	-
Ag_2O	-	<0.01	-	-
WO_3	<0.01	-	0.02	<0.01
Rock type	mafic	mafic	felsic	ultramafic
True depth (m)	44.4	46.1	44.9	34.2

Table 8. Minor element contents of pyrites (wt%), Mt Magnet

Sample No.	105103		108344		108348		108371			105144	
Drill hole/ Depth (m)	NMS D4: 70.8		NMS D7: 79.9		NMS D7: 103.8		NMS D8: 62.0			NMS D9: 73.6	
No. of analyses	6	7	5	6	2	5	5	4	3	3	6
Ag	0.01	0.01	0.01	<0.01	0.01	0.01	0.04	0.02	0.01	0.02	<0.01
As	0.44	0.02	0.15	0.01	<0.01	0.01	0.51	0.49	0.05	0.16	0.66
Co	0.14	0.02	0.04	<0.01	0.39	0.02	0.22	0.03	0.01	0.50	0.09
Cu	0.07	0.03	<0.01	<0.01	0.01	<0.01	0.02	0.02	0.02	0.17	0.33
Ni	0.29	0.16	0.07	0.01	0.02	0.03	0.30	0.07	0.03	0.46	0.03
Sb	0.03	0.01	0.03	<0.01	<0.01	<0.01	0.01	0.01	0.01	<0.01	0.03
Zn	<0.01	0.01	<0.01	0.01	0.01	0.01	0.01	0.01	0.04	0.01	0.04
Rock type	— mafic —		— felsic —		— mafic —		— felsic —			— mafic —	
Grain size (µm)	10-60	<20 (rim)	10-40	30 (rim) <500	10	5 (rim) ~20	10-50	20	<300	10-80	30-80
Pyrite type	I/II	III	II	III	I	III	I/II	II	III	I/II	II

Table 9. Compositions of carbonates (at%), Mt Magnet

Carbonate	Dol	Dol	Sid	Sid	Dol	Dol	Calc	Dol	Calc
Sample No.	105099	105103	105103	105103	108344	108348	108348	108371	108371
Drill hole	NMS D4	NMS D4	NMS D4	NMS D4	NMS D7	NMS D7	NMS D7	NMS D8	NMS D8
Depth (m)	58.3	70.8	70.8	70.8	79.9	103.8	103.8	62.0	62.0
No. of analyses	10	7	4	5	8	7	5	10	6
Ca	51.0	49.4	5.0	3.4	49.2	50.3	97.1	50.9	97.3
Mg	46.7	32.0	3.2	3.1	39.9	35.5	0.52	34.0	6.34
Fe	1.6	18.0	83.2	89.2	10.3	13.5	0.83	14.6	1.9
Mn	0.60	0.56	8.6	4.2	0.64	0.74	1.6	0.49	0.53
Mn/Fe	0.41	0.03	0.10	0.05	0.06	0.06	1.9	0.03	0.32
Rock type	mafic	mafic	mafic	mafic	felsic	mafic	mafic	felsic	felsic

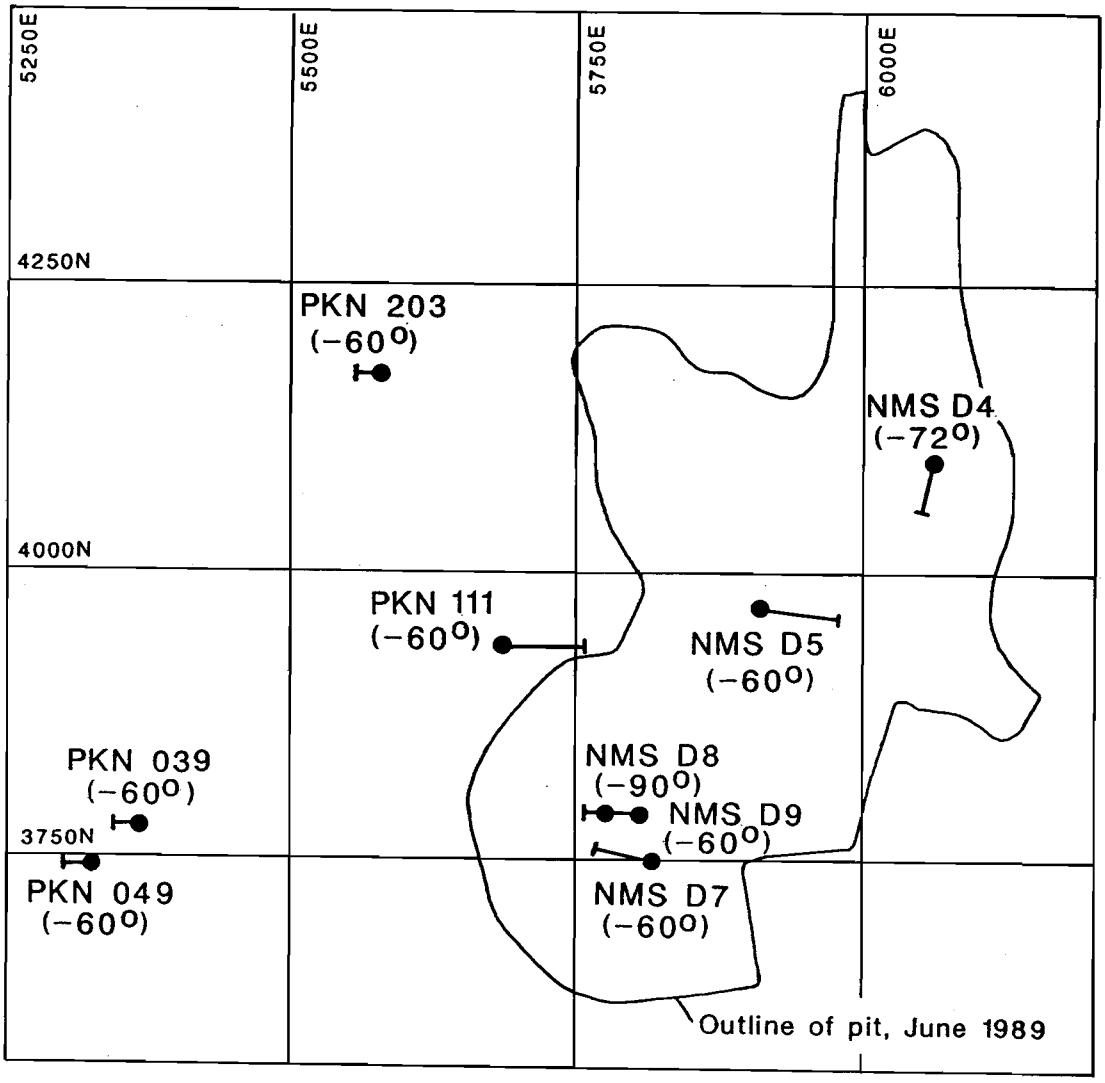

Figure 1 Location of studied drill holes, Parkinson Pit and environs, Mt Magnet.

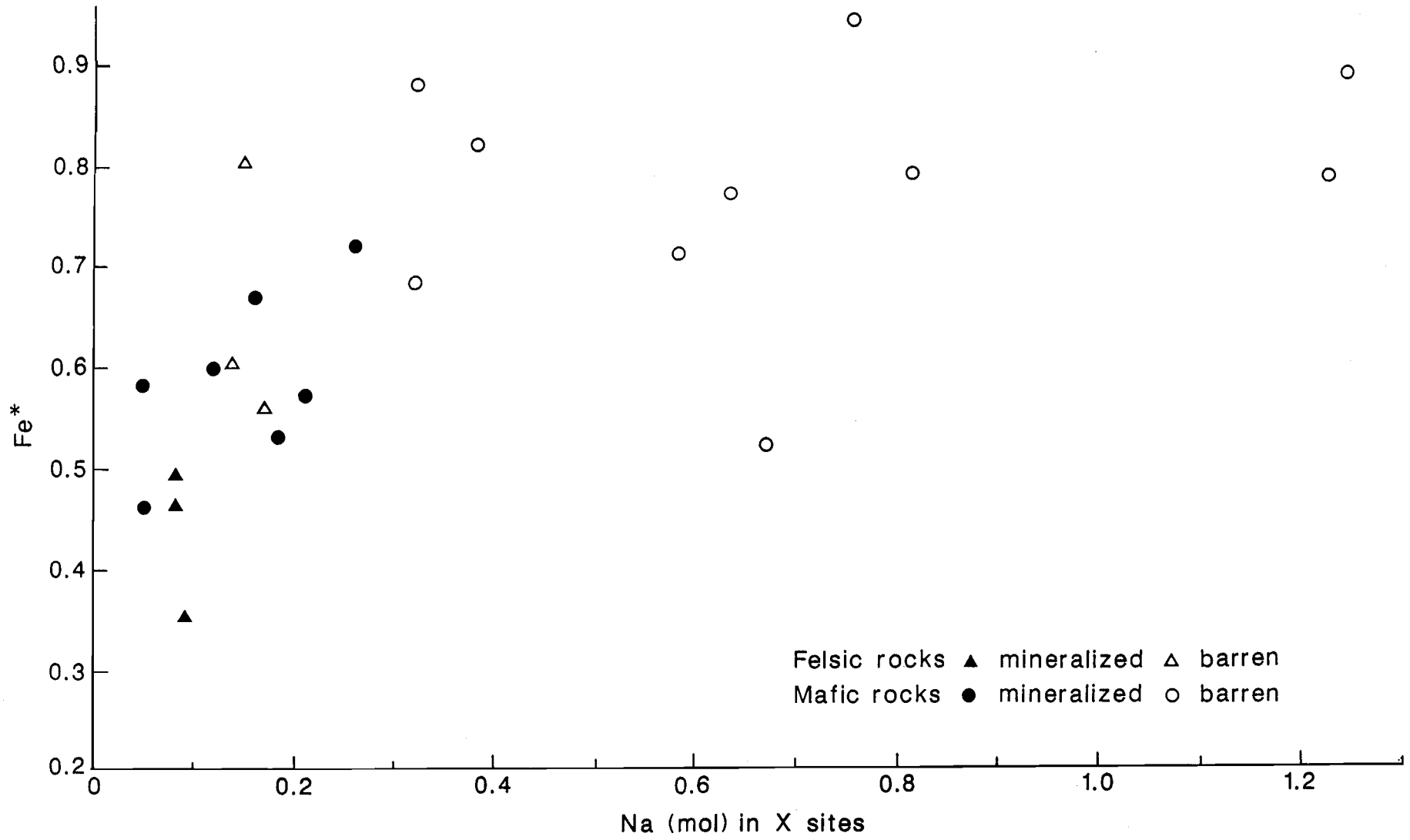

Figure 2 Na content of X sites vs Fe* for micas in mafic and felsic rocks, Mt Magnet.

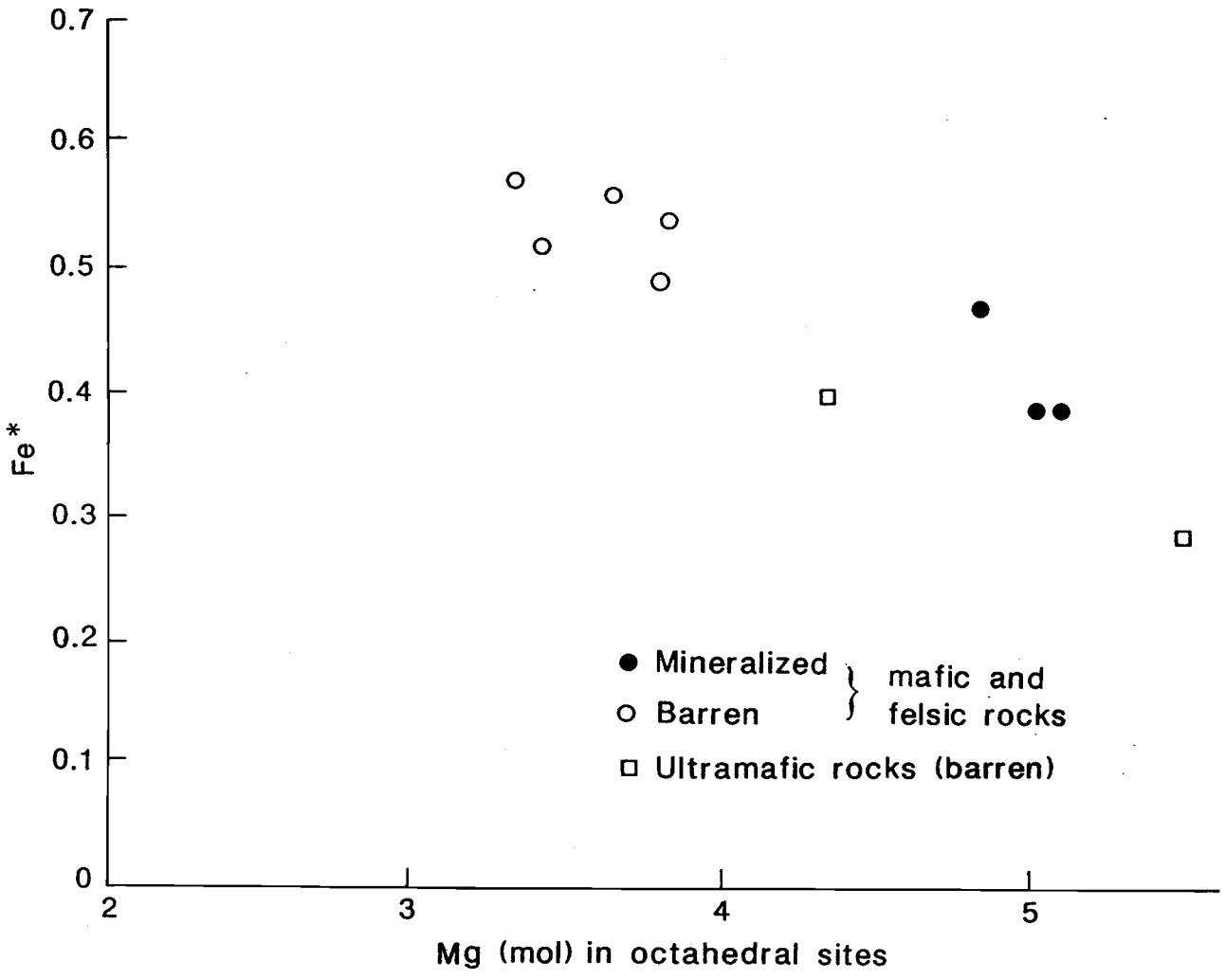

Figure 3 Mg content of octahedral sites vs Fe* for chlorites, Mt Magnet.

Figure 4 Hematite (light grey) rimmed by goethite (darker grey). Back Scattered Electron Image. Sample 105097. Scale ≡ 100 μm

Figure 5 Boxwork of cryptomelane (light grey), possibly after carbonate. Back Scattered Electron Image. Sample 108366. Scale ≡ 100 μm.

Figure 6 Fine stringer of secondary gold (white) in Fe oxide (grey). Back Scattered Electron Image. Sample 105073. Scale ≡ 10 μm.

Figure 7 Bleb of secondary gold (white) in void within Fe oxide (grey). Back Scattered Electron Image. Sample 105073. Scale ≡ 100 μm.

Figure 8 Primary (i.e.Ag-rich) gold grains (white) in chlorite matrix (grey). Back Scattered Electron Image. Sample 105099. Scale ≡ 100 μm.

Figure 9 Complex primary gold grain (white) associated with phyllosilicates (grey). Back Scattered Electron Image. Sample 105099. Scale ≡ 100 μm.

Figure 10 Au Mα map for Figure 9 area.

Figure 11 Ag Lα map for Figure 9 area, indicating Ag-rich core to upper portion of gold grain.

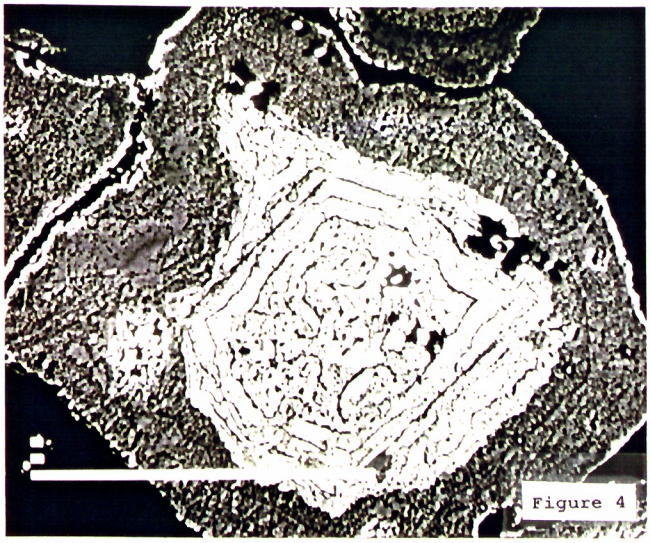

Figure 4

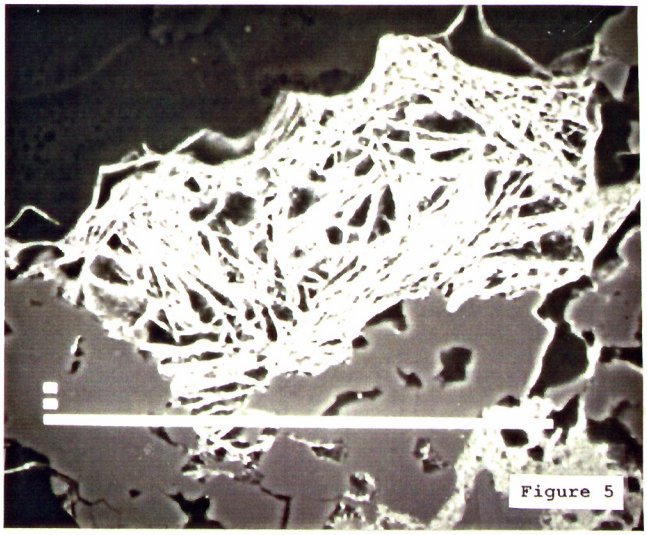

Figure 5

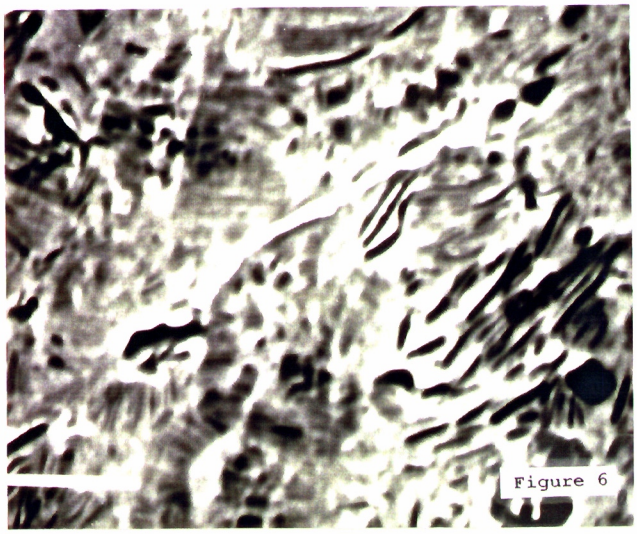

Figure 6

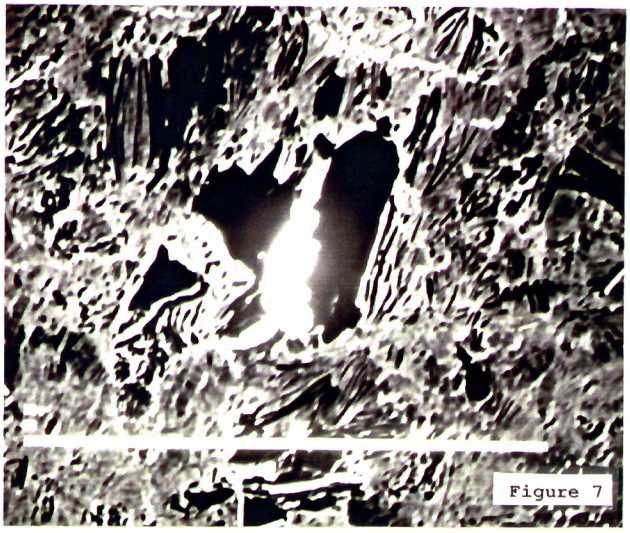

Figure 7

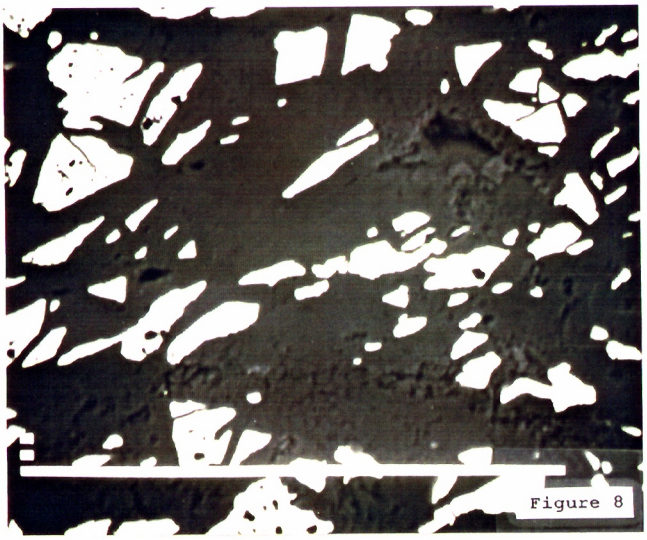

Figure 8

Figure 9

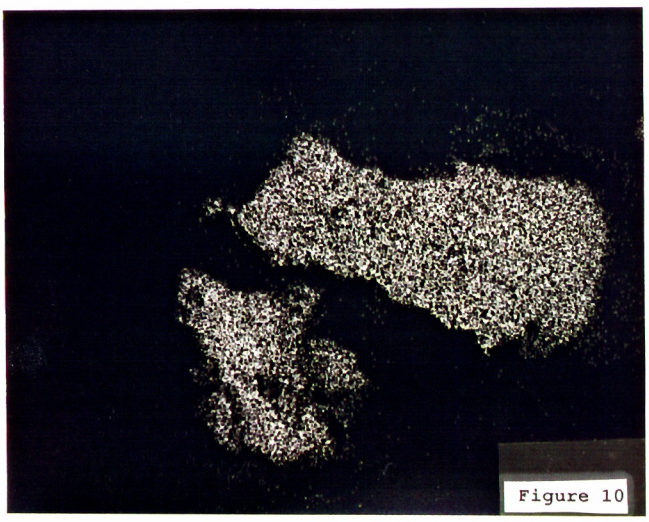

Figure 10

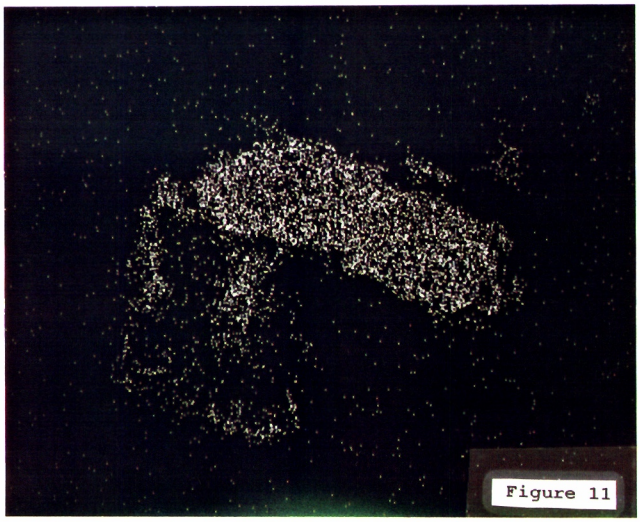

Figure 11